Pergamon

Corrosion Science, Vol. 38, No. 12, pp. 2121–2135, 1996

0010–938X/96 $15.00 + 0.00

PII: S0010–938X(96)00067–4

REVISED POURBAIX DIAGRAMS FOR IRON AT 25–300°C

B. BEVERSKOG and I. PUIGDOMENECH

Studsvik Material AB and Studsvik Eco and Safety AB, S-611 82 Nyköping, Sweden

Abstract—The Pourbaix diagrams, potential pH diagrams, for iron at 25–300°C have been revised. The selection of thermochemical data has taken into account the experimental solubility of magnetite at $T = 100$–300°C. Temperature extrapolations of thermochemical data for aqueous species have been performed with the revised Helgeson–Kirkham–Flower model, which also allows uncharged aqueous complexes to be handled. The Pourbaix diagrams show a stability region for ferrous hydroxide, $Fe(OH)_2(cr)$, at 10^{-6} m and $T \leq 85$°C, implying that the Schikorr reaction is not thermodynamically possible above this temperature. A corrosion region between iron and magnetite exists at all temperatures in high purity water (10^{-8} m), due to the hydrolysis products of iron(II).

INTRODUCTION

Equilibrium calculations show whether a chemical or electrochemical reaction may proceed or not. No information is given about the rate of the reaction, i.e. its kinetics. However, increasing temperature and thereby usually faster reaction rates, cause diagrams based on only thermodynamic considerations to be more relevant.

A Pourbaix diagram, or potential pH diagram, is a map of thermodynamic possibilities. The Pourbaix diagram can be seen as a map in the chemical space, summarizing thermodynamic information in a compact and at the same time useful way.

There are numerous publications on Pourbaix diagrams for the system iron–water.[1–55] However, most workers have uncritically used the species that Pourbaix used in his 1945 thesis.[1] Since the study by Pourbaix, new findings make it relevant to once again revise the Pourbaix diagram for iron.

All earlier publications of Pourbaix diagrams for iron at elevated temperatures[9–13,15,29–31,33,35,36,38,40,42,46,50,53,55] have been based on the correspondence principle of Criss and Cobble,[56] with one exception[10] where the method of deBethune *et al.*[57,58] has been used. However, the correspondence principle of Criss and Cobble is equivalent to a linear dependency of S° with temperature for an aqueous species, while the equations of deBethune *et al.* imply that values of $\Delta_r S^\circ$ are T-independent. For temperatures above 150°C neither of these approximations is adequate, and electrostatic models such as that developed by Tanger and Helgeson,[59] Shock *et al.*[60] and Shock and Helgeson[61] fit better the experimental dependency of the heat capacity of an aqueous species with temperature. There is no study in the literature reporting Pourbaix diagrams for iron on activity lower than 10^{-6} for dissolved species. However, as the contamination is low in high purity water, such as the cooling media in nuclear reactors of the boiling water type, this work

Manuscript received 15 March 1996; accepted 2 May 1996.

has been performed not only for the conventional 10^{-6}, but also for 10^{-8} m concentrations.

The solubility of magnetite (Fe_3O_4(cr)) at high temperatures is well established, *cf.*[62] and references therein. However, most of the earlier published Pourbaix diagrams for elevated temperatures have not used thermochemical data adjusted to take into account the experimental solubility of magnetite. The diagrams by Cubicciotti[50] set the predominance of magnetite (at pH$\geq$6 at $p_{H_2(g)} \approx 1$ atm and 290°C), close to the experimental results of Tremaine and LeBlanc[63] ($[Fe]_{TOT} = 10^{-6}$ M at pH 5 and 300°C), but the Pourbaix diagrams in Cubicciotti[50] are unsatisfactory because anionic hydrolysis products were not included. The diagrams by Chen and Aral[37] and Chen *et al.*[38] show also a correct pH range for the predominance of magnetite, but they (among others) did not include the $Fe(OH)_4^-$ complex, resulting in a distorted predominance area for hematite in alkaline media.

Owing to the shortcomings in previously published Pourbaix diagrams at elevated temperatures, this work was started with the aim to revise the Pourbaix diagrams for the iron–water system up to 300°C, using thermochemical data in accordance with the experimental stability of magnetite [including the first four hydrolysis complexes of Fe(II) and Fe(III)], and using appropriate methods for the temperature extrapolation of thermochemical data.

SOLIDS AND AQUEOUS SPECIES OF IRON

Iron has the electron configuration $[Ar]3d^64s^2$. The relatively low energy in the s- and d-levels makes it possible for iron to have the oxidation numbers 0–VI. The most common oxidation numbers for iron in water solutions are II and III. Strongly alkaline solutions can contain iron(IV) and iron(VI). The oxidation numbers −II, −I, 0 and I are usually not stable in aqueous solutions. Acid solutions of iron(II) contain the Fe^{2+} ion, which hydrolyses to $FeOH^+$ and $Fe(OH)_2$(aq) in neutral solutions and may precipitate as $Fe(OH)_2$(s). In alkaline solutions anionic complexes, such as $Fe(OH)_3^-$ and $Fe(OH)_4^{2-}$, are formed. For iron(III) the aqueous complex Fe^{3+} is formed in very acidic solutions, and it hydrolyses easily as pH increases to $FeOH^{2+}$, $Fe(OH)_2^+$, $Fe(OH)_3$(aq), and several polynuclear complexes like $Fe(OH)_2^{4+}$ and $Fe(OH)_4^{5+}$. $Fe(OH)_3$ precipitates in neutral solutions, but the solubility increases again in very alkaline solutions through formation of $Fe(OH)_4^-$.

The hydrolysed anionic ferrous complexes in alkaline solutions are denoted as $Fe(OH)_3^-$ and $Fe(OH)_4^{2-}$ and not with the traditional notation of $HFeO_2^-$ and FeO_2^{2-} generally used in Pourbaix diagrams. The difference is only one or two water molecules. This is also in agreement with the nomenclature used by Baes and Mesmer[64] and Tremaine and LeBlanc.[63] $Fe(OH)_3^-$ and $Fe(OH)_4^{2-}$ are consistent with the ferrous hydrolysis series, where every hydrolysis step adds a hydroxide ion.

Table 1 shows the 32 iron species that have been considered in the aqueous iron system. Of these, six solid phases and 11 dissolved species have been included in our calculations, while 10 solids and five dissolved species were excluded. In accordance with Pourbaix, the $Fe(OH)_4^{2-}$ ion is included with a question mark.[1,21] This ion may exist in very alkaline solutions, but it is unstable in neutral and acidic solutions.[65]

$Fe_{1-x}O$ (wustite) was not considered as it is not stable below 570°C.[65,66] The stoichiometric monoxide is not thermodynamically stable either. Thermochemical data is missing for hydrated magnetite as well as for the Fe(IV) species. γ-Fe_2O_3 (maghemite) and

Table 1. Considered iron species in the iron–water system

Condition	Oxidation number	Included	Excluded
Crystalline	0	Fe	
Crystalline	II	$Fe(OH)_2$	$Fe_{1-x}O$
Crystalline	II		FeO
Crystalline	II/III	α-Fe_3O_4	$Fe_3O_4 \cdot H_2O$
Crystalline	II/III		γ-Fe_3O_4
Crystalline	III	$Fe(OH)_3$	β-FeOOH
Crystalline	III	α-FeOOH	γ-FeOOH
Crystalline	III		δ-FeOOH
Crystalline	III		δ'-FeOOH
Crystalline	III		$Fe_5HO_8 \cdot H_2O$
Crystalline	III	α-Fe_2O_3	γ-Fe_2O_3
Dissolved	II	Fe^{2+}	
Dissolved	II	$FeOH^+$	
Dissolved	II	$Fe(OH)_2(aq)$	
Dissolved	II	$Fe(OH)_3^-$	
Dissolved	II	$Fe(OH)_4^{2-}$	
Dissolved	III	Fe^{3+}	
Dissolved	III	$FeOH^{2+}$	
Dissolved	III	$Fe(OH)_2^+$	
Dissolved	III	$Fe(OH)_3(aq)$	
Dissolved	III	$Fe(OH)_4^-$	
Dissolved	III		$Fe(OH)_4^{2+}$
Dissolved	III		$Fe(OH)_5^{4+}$
Dissolved	IV		FeO^{2+}
Dissolved	IV		FeO_3^{2-}
Dissolved	V		FeO_2^+
Dissolved	VI	$Fe(OH)_4^{2-}$	
Σ		6 + 11 = 17	10 + 5 = 15

the oxyhydroxides of Fe(III) are all thermodynamically unstable with the respect to hematite and they would not appear in the results of thermodynamic equilibrium calculations unless the formation of more the stable solid phases is suppressed. The aqueous Fe(IV) and Fe(V) ions have not been considered because of their instability in aqueous solutions. Polynuclear hydrolysis complexes of Fe(III) form only at high concentrations of dissolved iron[64] and not at the concentrations used in this work, and therefore these complexes have been neglected here.

THERMOCHEMICAL DATA

A critical review of published thermochemical data has been performed for the solids and aqueous species described in previous Section. Data is usually available only for a reference temperature of 25°C in the form of standard molar Gibbs free energy of formation from the elements ($\Delta_f G°$) and standard molar entropy ($S°$). Equations for the temperature dependence of the standard molar heat capacity ($C_p°$) are usually available for solid and gaseous compounds. For aqueous species, the standard partial molar properties are usually available. Extrapolation of thermochemical data to other temperatures is performed with

Table 2. Thermodynamic data at 25°C for the system iron–water

Species	$\Delta_f G^\circ$ (kJ mol^{-1})	S° (J K^{-1} mol^{-1})	$C_p^\circ T/(\text{J K}^{-1}\text{ mol}^{-1}) = a + bT + cT^{-2}$		
			a†	$b \times 10^3$	$c \times 10^{-6}$
Fe(cr)	0.	27.28	28.18	−7.32	−0.290‡
Fe_3O_4(cr)	−1012.57	146.14	2659.108	−2521.53	20.7344§
α-Fe_2O_3(cr)	−744.3	87.40	−838.61	−2343.4¶	
$Fe(OH)_2$(cr)	−491.98	88.	116.064	8.648	−2.874
α-FeOOH(cr)	−485.3	60.4	49.37	83.68	
$Fe(OH)_3$(cr)	−705.29	106.7	127.612	41.639	−4.217
Fe^{2+}	−91.88	−105.6	−2		
$FeOH^+$	−270.80	−120	450		
$Fe(OH)_2$(aq)	−447.43	−80	435		
$Fe(OH)_3^-$	−612.65	−70	560		
$Fe(OH)_4^{2-}$	−775.87	−170	600		
Fe^{3+}	−17.59	−276.94	−143		
$FeOH^{2+}$	−242.23	−118	50		
$Fe(OH)_2^+$	−459.50	8	230		
$Fe(OH)_3$(aq)	−660.51	30	365		
$Fe(OH)_4^-$	−842.85	45	300		
$Fe(OH)_4^{2-}$	−322	37.7	−212		

† For aqueous species 'a' corresponds to the standard partial molar heat capacity at 25°C, and the revised Helgeson–Kirkham–Flowers model has been used to obtain its temperature dependence.

‡ $C_p^\circ(\text{Fe(cr)},T)/(\text{J K}^{-1}\text{ mol}^{-1}) = a + bT + cT^{-2} + dT^2$, with $d = 25.04 \times 10^{-6}$.

§ $C_p^\circ(\text{magnetite},\ T)/(\text{J K}^{-1}\text{ mol}^{-1}) = a + bT + cT^2 + dT^{-2} + eT^{-0.5}$, with $d = 1.36769 \times 10^{-3}$, and $e = -3.645541 \times 10^4$.

¶ $C_p^\circ(\text{hematite},\ T)/(\text{J K}^{-1}\text{ mol}^{-1}) = a + bT + dT^2 + fT^{0.5} + gT^{-1}$, with $d = 6.0519 \times 10^{-4}$, $f = 86.525$, and $g = 2.7821 \times 10^4$.

the methodology described later in Calculations. For aqueous species our methodology requires a value of C_p° at 25°C.

The data selected for the calculations performed in this report are summarized in Table 2. The selection criteria behind the values in this table are discussed below.

SOLIDS

The standard Gibbs free energy of formation for Fe(cr) is by definition zero at all temperatures. The value of S° selected in this work for elemental iron is that listed in the NBS tables,[67] while parameters for the temperature equation of the heat capacity are taken from Kubaschewski.[68] Values of $\Delta_f G^\circ$ and S° for magnetite and hematite are those given in Hemingway,[69] and the $C_p^\circ(T)$ equations for these solids are those from Hemingway[69] and Robie *et al.*,[70] respectively. It must be noted that the values for magnetite constitute the basis for many of the data for the aqueous hydrolysis species of both Fe(II) and Fe(III) as discussed below. For α-FeOOH(cr), the data given in Kubaschewski[68] have been used.

For $Fe(OH)_2$(cr), the values of $\Delta_f G^\circ$ and S° are from Knacke *et al.*[71] The value of $\Delta_f G^\circ$ for $Fe(OH)_3$(cr) has been calculated from the solubility product selected by Nordstrom *et*

al.,[72] while the value of S° is from the NBS tables.[67] The $C_p^\circ(T)$ equations for these two hydroxides have been taken from Knacke *et al.*[71]

AQUEOUS SPECIES

The thermodynamic properties of $H_2O(l)$ at 25°C recommended by CODATA[73] have been used in this work. The temperature dependence of these properties has been calculated with the model described by Saul and Wagner.[74] The dielectric constant of water (which is needed for the revised Helgeson–Kirkham–Flowers model that describes the temperature dependence of the thermodynamic properties of aqueous solutes, as discussed below) has been obtained with the equations given in Archer and Wang.[75]

Following Helgeson,[76] the values of S° and $\Delta_f G^\circ$ for Fe^{2+}, which is a key species in this system, are calculated from the data of Larson *et al.*[77] on the heat of solution of $FeSO_4 \cdot 7H_2O(cr)$, using values from CODATA[73] for SO_4^{2-} and $H_2O(l)$, resulting in slightly different values of S°, $\Delta_f H^\circ$ and $\Delta_f G^\circ$ than those calculated by Larson *et al.*[77] The standard partial molar heat capacity reported by Bernarducci *et al.*[78] has been used here.

For Fe^{3+}, which is also a key species in this system, the values of S° and $\Delta_f G^\circ$ are derived from the Fe^{2+} data and the standard redox potential and $\Delta_r S^\circ$ for the Fe^{3+}–Fe^{2+} couple reported in Whittemore and Langmuir.[79] This procedure is the same as that followed in Helgeson[76] and Heusler and Lorenz.[80] The value of $C_p^\circ(Fe^{3+})$ is taken from Shock and Helgeson[61], where approximately the same value for $S^\circ(Fe^{3+}, 25°C)$ is given as that in Table 2.

Values of $\Delta_f G^\circ$ for the hydrolysis products of Fe(II) and Fe(III) have been calculated from the values of $\Delta_f G^\circ$ for Fe^{2+} and Fe^{3+} and from the equilibrium constants at 25°C for the general hydrolysis reactions:

$$Fe^{2+} + mH_2O(l) \rightleftarrows Fe(OH)_m^{(2-m)} + mH^+, \quad (1)$$

$$Fe^{3+} + nH_2O(l) \rightleftarrows Fe(OH)_n^{(3-n)} + nH^+, \quad (2)$$

obtained by Tremaine and Leblanc[63] (for $FeOH^+$, $Fe(OH)_2(aq)$ and $Fe(OH)_3^-$) and selected by Baes and Mesmer[64] (for all other hydrolysis complexes). The slightly better fit of the temperature dependence of magnetite solubility with the values for the Fe(II) complexes given by Tremaine and LeBlanc[63] has been the reason for using these equilibrium constants instead of the the data selected by Baes and Mesmer.[64]

The values of S° and C_p° for $FeOH^+$, $Fe(OH)_2(aq)$, $Fe(OH)_3^-$, $Fe(OH)_3(aq)$ and $Fe(OH)_4^-$ have been calculated from the T-dependence of the magnetite solubility reported by Tremaine and LeBlanc[63] in aqueous solutions containing molecular hydrogen and different acidities/alkalinities. Figure 1 shows a comparison between experimental magnetite solubilities and those calculated with the data in Table 2. The larger discrepancies can be found at 100°C and low pH values. It should be noted that the data at low pH values, where Fe^{2+} predominates in the aqueous solution (pH less than ~4 at 300°C and pH less than ~7 at 100°C), correspond to predictions of magnetite solubilities calculated according to

$$1/3Fe_3O_4(cr) + 1/3H_2(g) + 2H^+ \rightleftarrows Fe^{2+} + 4/3H_2O(l),$$

because all the thermochemical data for all the reactants and products in this reaction

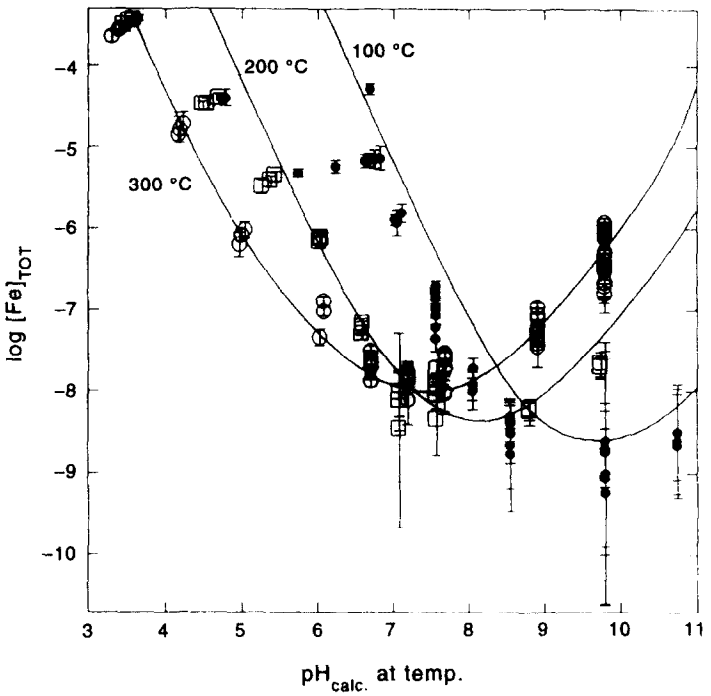

Fig. 1. Comparison between calculated and experimental[63] solubilities of magnetite in aqueous solutions containing $[H_2(aq)] = 779\ \mu mol\ kg^{-1}$.

have been determined independently to the experimental solubilities in Tremaine and LeBlanc.[63]

The selected values of S° and C_p° for these aqueous species ($FeOH^+$, $Fe(OH)_2(aq)$, $Fe(OH)_3^-$, $Fe(OH)_3(aq)$ and $Fe(OH)_4^-$) should be considered as fitting parameters, with perhaps little physico-chemical significance. Their absolute values depend on five main factors: (a) the experimental data fitted; (b) the mathematical model used to describe the temperature dependence of C_p°; (c) the thermodynamic properties [$\Delta_f G^\circ$, S° and C_p° (T)] of magnetite and Fe^{2+}; (d) the iron speciation assumed for the aqueous phase; and (e) the values of $\Delta_f G^\circ$ at 25°C for these species. Among the differences between our fitting procedure and that used by Tremaine and LeBlanc[63] is the fact that the enthalpy change for equation (1) with $m = 1$, for the formation of $FeOH^+$ ($\Delta_r H^\circ = 33\ kJ\ mol^{-1}$ as calculated from the data of Table 2) has not been constrained here to the experimental values reported at 25°C ($\Delta_r H^\circ = 50\ kJ\ mol^{-1}$ [81] and $\Delta_r H^\circ = 36\ kJ\ mol^{-1}$ [82]).

The value of S° ($FeOH^{2+}$) has been selected to yield $\Delta_r H^\circ = 39\ kJ\ mol^{-1}$ for equation (2) with $n = 1$ (the average of the value at $I = 0$ quoted elsewhere[64,83] and the value obtained from the T-dependency of the equilibrium constants[84]).

It should be noted that the values of $\Delta_f G^\circ$ (300°C) calculated by extrapolating the data in Table 2 agree only within ± 2 $\log K_{eq}$ units with the values obtained by Zeng *et al.*[85] in their analysis of the experimental solubility of the magnetite + hematite assemblage in sodium chloride solutions at 300°C and 500 bars:

$$\frac{1}{6}Fe_3O_4(cr) + \frac{1}{4}Fe_2O_3(cr) + H^+ + \frac{5}{12}H_2(g) \rightleftarrows \frac{5}{12}H_2O(l) + FeOH^+,$$

$\log K°_{eq} = 0.85;^{85}$ -0.95 (calculated from Table 2),

$$\frac{1}{6}Fe_3O_4(cr) + \frac{1}{4}Fe_2O_3(cr) + \frac{19}{12}H_2O(l) \rightleftarrows \frac{1}{12}H_2(g) + Fe(OH)_3(aq),$$

$\log K°_{eq} = -7.32;^{85}$ -8.42 (calculated from Table 2),

$$\frac{1}{6}Fe_3O_4(cr) + \frac{1}{4}Fe_2O_3(cr) + \frac{31}{12}H_2O(l) \rightleftarrows \frac{1}{12}H_2(g) + H^+ + Fe(OH)_4^-,$$

$\log K°_{eq} = -16.02;^{85}$ -16.39 (calculated from Table 2).

No experimental data has been found for the remaining thermodynamic values required in the aqueous Fe(II) and Fe(III) systems, and these data have been estimated as follows. The value of $S°$ for $Fe(OH)_2^+$ has been set to obtain a smooth variation of $\Delta_r H°$ against 'n' for equation (2). Values of $C_p°$ for $FeOH^{2+}$ and $Fe(OH)_2^+$ have also been set to obtain a smooth variation of $\Delta_r C_p°$ against 'n' in equation (2) between Fe^{3+} ($\Delta_r C_p° = 0$) and $Fe(OH)_3(aq)$ ($\Delta_r C_p°$ determined for magnetite solubility). The values of $S°$ and $C_p°$ for $Fe(OH)_4^{2-}$ have been adjusted to avoid the predominance of this species over the pH and temperature ranges studied by Tremaine and LeBlanc.[63]

There are no precise data for the ferrate ion. Pourbaix and de Zoubov[4] give a 'provisional' value of $\Delta_f G°(FeO_4^{2-}) = -467\ kJ\ mol^{-1}$, and this value has been used later for the construction of the majority of the Pourbaix diagrams of iron. Wood[86] determined experimentally $\Delta_f H°(FeO_4^{2-}) = -481\ kJ\ mol^{-1}$ and estimated a value of $S°(FeO_4^{2-}) = 37.7\ J\ K^{-1}\ mol^{-1}$, resulting in $\Delta_f G° = -322\ kJ\ mol^{-1}$ for this ion, and these values, which later have been quoted by Misawa[20] and Charlot *et al.*,[87] are selected here. The value of $C_p°$ (FeO_4^{2-}) has been estimated to be the average of the values for CrO_4^{2-}, MoO_4^{2-} and WO_4^{2-} given in Shock and Helgeson.[61]

CALCULATIONS

For solids and gaseous compounds temperature effects have been obtained by the standard integration of the heat capacity temperature equations. Extrapolation of thermochemical data of aqueous species to higher temperatures has been performed with the revised Helgeson–Kirkham–Flowers model.[59–61,88] However, some simplifications are needed to use this model when only the value of $C_p°$ (25°C) is available. For each aqueous species, the value of $C_p°$ (25°C) and the value of $S°$(25°C) are used to estimate the parameters in the revised Helgeson–Kirkham–Flowers model: c_1, c_2 and ω, *cf.* equations (29), (31), (35), (45), (56), (57) and (89) in Shock and Helgeson[61] and equations (21), (23), (26), (44) and (45) in Shock *et al.*[88] This allows first the calculation of the apparent standard partial molar Gibbs free energy of formation of aqueous species participating in a chemical reaction at higher temperatures, and then the equilibrium constant of the reaction as a function of T, *cf.* equations (93) and (94) in Shock and Helgeson.[61]

Chemical equilibrium diagrams (including Pourbaix diagrams), have been drawn with computer software[89] using the chemical compositions calculated with the SOLGASWATER algorithm,[90] which obtains the chemical composition of systems with an aqueous solution and several possible solid compounds by finding the minimum of the

Gibbs free energy of the system. The technique employed to draw the diagrams consists of calculating chemical equilibria compositions in a 200 × 200 grid with consequent drawing of stability areas for solids and predominance areas for aqueous species. This technique has the drawback of being time-consuming and producing diagrams of limited resolution, but the resulting diagrams are more accurate than those obtained with the traditional method of comparing equilibrium constants and E_{SHE}/pH slopes.

Calculations to draw the Pourbaix diagrams presented in this work have been performed for eight temperatures in the interval 25–300°C (25, 50, 100, 150, 200, 250, 285 and 300°C).

The concentration of dissolved metallic species used in Pourbaix diagrams is, if not specified, 10^{-6} M. The value was stipulated by Pourbaix as the limit for practical corrosion. At concentrations of dissolved metallic species $>10^{-6}$ M the metal is considered to corrode and at concentrations $<10^{-6}$ M the metal is considered not to corrode. This boundary value is a definition for aqueous corrosion that is useful for practical applications.

Pourbaix diagrams have been calculated in this work at two concentration levels, 10^{-6} and 10^{-8} M at each temperature. The former is the conventional corrosion limit and the latter is intended to be used in high purity waters, such as the cooling media in nuclear reactors of the boiling water type. These concentrations are total concentrations, i.e. the sum of all aqueous species containing iron at each coordinate point (E_{SHE}/pH-value). Because they are temperature-independent, molal concentration units (mol (kg of water)$^{-1}$) are used in the calculations.

Activity factors for aqueous species have been neglected in the construction of the Pourbaix diagrams, and similarly the activity of water has been fixed to unity. This is in agreement with the frequently used assumption when drawing and using chemical equilibria diagrams that thermodynamic activity may be used instead of concentration. However, this does not hold for concentrated solutions, for example those with very low or high pH. The activity coefficient of these solutions will probably be large and will change quickly with pH, and concentration ratios might deviate strongly from the corresponding activity ratios obtained from the thermodynamic equations. For this reason, lines in chemical equilibrium diagrams based on activity ratios might lack significance,when the lines are below pH $\approx$ 1 and beyond pH $\approx$ 13. The lines in these regions, which should perhaps be dashed, have been included in this work due to reasons of construction.

The electrochemical potentials reported in this work are always related to the standard hydrogen electrode (E_{SHE}), which is considered to be zero at all temperatures.

The parallel sloping dotted lines in the Pourbaix diagrams limit the stability area of water at atmospheric pressure of gaseous species. The upper line represents the oxygen equilibrium line ($O_2(g)/H_2O$)1)) and potentials above this line will oxidize water with oxygen evolution. The lower line represents the hydrogen line ($H^+/H_2(g)$) and potentials below this line will result in hydrogen evolution.

All values of pH given in this work are values at the specified temperature. The neutral pH value of pure water changes with the temperature with the ion product of water ($H_2O(l) \rightleftarrows H^+ + OH^-$), $pH_{neutral} = 1/2\, pK_{W,T}$). To facilitate reading of the Pourbaix diagrams, the neutral pH value at the temperature of each diagram is given as a vertical dotted line, and the pH scale in the diagrams is limited by the pK_W value (pK_W = 12.3, 11.3; 11.3 at T = 100, 200 and 300°C, respectively).

EXPERIMENTAL RESULTS AND DISCUSSION

The thermochemical data for solid compounds listed in Table 2 agree in general with those listed in other complications, and our $\Delta_f G^\circ$ values for the aqueous hydrolysis species are non-controversial as well. The selection of entropy (and enthalpy) changes for reactions involving aqueous species depends among other things on the equations used for the temperature variation of C_p° for aqueous solutes, and therefore several of the S° and C_p° values selected in this study for aqueous species differ substantially from those in other compilations. Thus S° values for Fe(II) and Fe(III) species in Table 2 differ by as much as ± 120 and $\pm 105\,J\,K^{-1}\,mol^{-1}$, respectively with those in Pourbaix *et al.*[33] Similar discrepancies can be found between our entropy data for aqueous iron species and those in other compilations.[91,92] It must be noted, however, that there are disagreements among these other compilations, even in the values of S° for the Fe^{3+} and Fe^{2+} ions. As noted above, the S° and C_p° values for hydrolysis complexes listed in Table 2 should perhaps be regarded as fitting parameters, which adequately describe the temperature dependence of the solubility of magnetite, and therefore these are well suited for the calculation of Pourbaix diagrams at elevated temperatures.

The diagram at 300°C and 10^{-8} M shows a predominance area for haematite set against the $Fe(OH)_3$(aq) field, Fig. 3. However, the thermochemical data selected for this complex is not well constrained by the fit of the solubility of magnetite, because the two neutral hydrolysis complexes, $Fe(OH)_2$(aq) and $Fe(OH)_3$(aq), compete with each other and at this temperature these have only a minor contribution to the total iron concentration. Furthermore, an experimental study on the solubility of haematite[93] at 300°C shows the minimum Fe(III) concentration at $10^{-6.04}$ M, indicating that the appearance of a stability area for haematite at 300°C at 10^{-8} M is perhaps an artefact of our calculations.

The decreasing range of existence of magnetite in the Pourbaix diagrams as the temperature increases shown in Figs 2 and 3 is well in accordance with the extensive experimental evidence on the solubility of Fe_3O_4(cr),[62] as illustrated in Fig. 1.

Two general remarks can be made regarding the temperature and concentration dependence of the calculated diagrams. Firstly, temperature changes the size of the different stability areas of immunity, passivity and corrosion. Both the immunity area (stability of the metal itself) and the passivity area (stability of solid compounds) decrease with increasing temperature. The corrosion area (stability of dissolved species) at acidic pH decreases, while the corrosion area at alkaline pH increases with increasing temperature. The reason for this behaviour is related to the temperature dependence of the ion product of water. Secondly, the concentration of dissolved species also changes the size of the different stability areas. The immunity and passivity areas increase with increasing concentration, resulting in a decrease of the corrosion area.

The results of the original thermodynamic calculations performed in 1991 are summarized in 24 diagrams in an internal technical report,[94] but as all these can not be included in this paper, the results are condensed in Table 3.

The Pourbaix diagrams for iron show a base metal, as the immunity region is situated below the hydrogen–water line, Figs 2 and 3. However, iron can passivate in slightly alkaline solutions, where a solid layer protects the metal from further dissolution (the ideal case).

Acidic solutions dissolve iron and form Fe^{2+}(aq) with hydrogen evolution. At

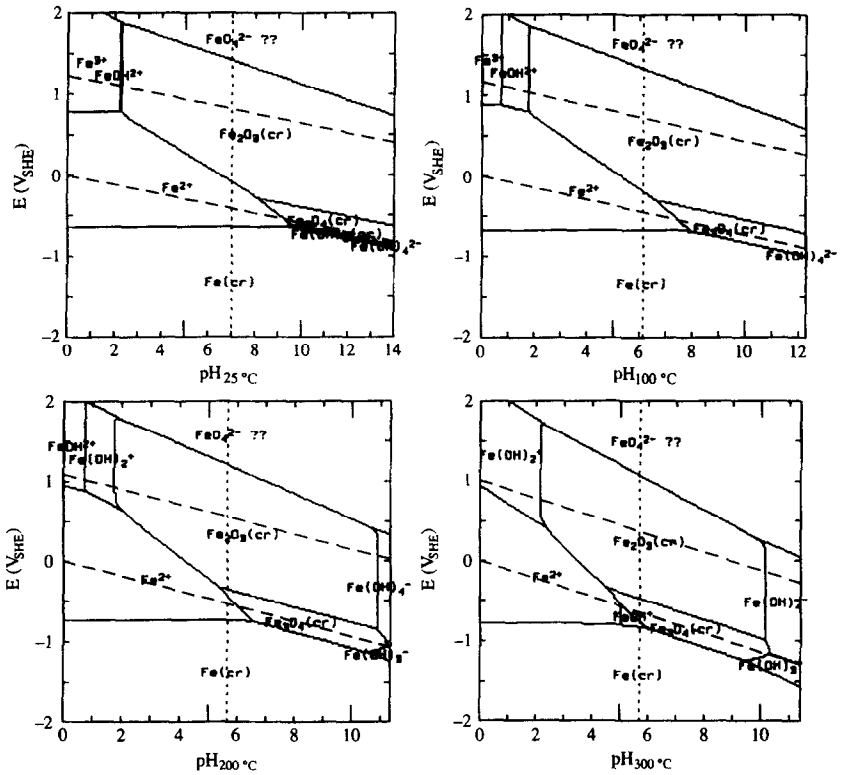

Fig. 2. Pourbaix diagrams for iron at 10^{-6} m at 25, 100, 200 and 300°C.

concentrations of 10^{-6} M the first ferrous hydrolysis product, $FeOH^+(aq)$, predominates at high temperatures (250–300°C), Fig. 2. This complex predominates at all temperatures at the concentration of 10^{-8} M, Fig. 3.

Passivity for iron is achieved in alkaline solutions, see Figs 2 and 3. Ferrous hydroxide $Fe(OH)_2(cr)$ forms at low temperatures with a narrow stability area (Fig. 2). This result is in fair agreement with Pourbaix *et al.* at 25°C,[33] and Le and Gali.[55] The decomposition of iron(II) hydroxide into magnetite and iron,

$$4Fe(OH)_2(cr) \rightarrow Fe_3O_4(cr) + Fe(cr) + 4H_2O(l),$$

takes place according to the data in Table 2 at $T \geq 85$°C, although there is a considerable uncertainty in this value (perhaps ± 20°C). Ferrous hydroxide has higher solubility than magnetite, haematite or goethite,[95] and our calculations explain the experimental results of a weak corrosion region between iron and magnetite which is pointed out by Pourbaix, although he gave no explanation.

Iron in de-aerated aqueous solution becomes passivated by the formation of a protecting layer of magnetite. According to Schikorr the reaction goes through the formation of iron(II) hydroxide as an intermediate between elementary iron and magnetite.[96,97] The reaction is called the Schikorr reaction and is written as

$$3Fe(OH)_2(cr) \rightarrow Fe_3O_4(cr) + H_2(g) + 2H_2O(l),$$

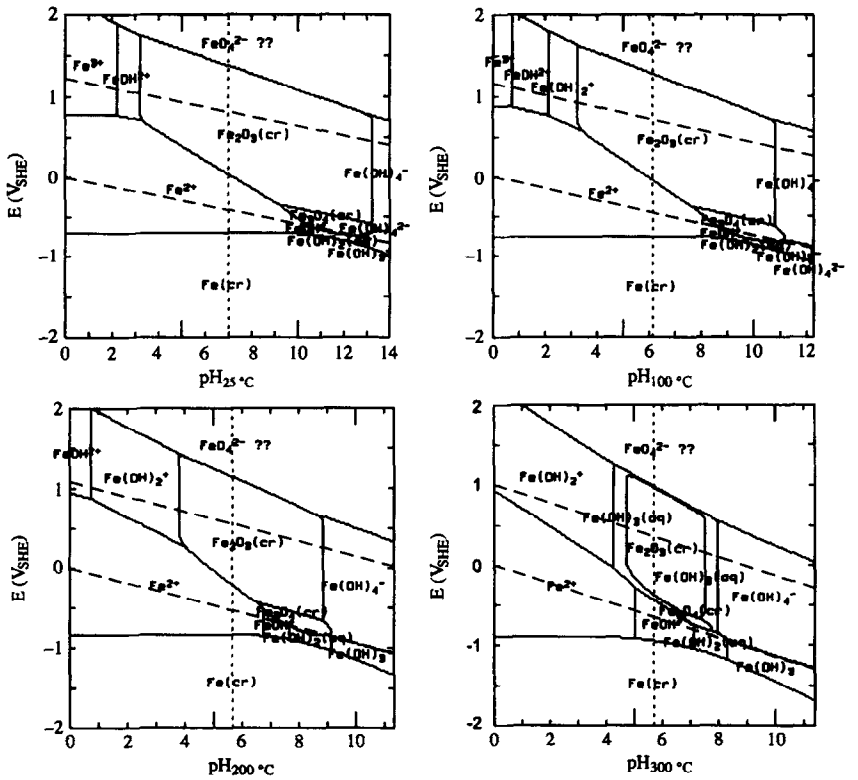

Fig. 3. Pourbaix diagrams for iron at 10^{-8} m at 25, 100, 200 and 300°C.

Table 3. Calculated thermodynamic stability of iron species in the system of iron–water. (P = predominates at 10^{-6} M; p = predominates at 10^{-8} M; d = appears in the predominance diagram for dissolved species)

Species	25°C	50°C	100°C	150°C	200°C	250°C	285°C	300°C
Fe(cr)	P p -	P p -	P p -	P p -	P p -	P p -	P p -	P p -
$Fe(OH)_2$(cr)	P - -	P - -	- - -	- - -	- - -	- - -	- - -	- - -
Fe_3O_4(cr)	P p -	P p -	P p -	P p -	P p -	P p -	P p -	P p -
α-Fe_2O_3(cr)	P p -	P p -	P p -	P p -	P p -	P p -	P p -	P p -
Fe^{2+}(aq)	P p d	P p d	P p d	P p d	P p d	P p d	P p d	P p d
$FeOH^+$(aq)	- p d	- p d	- p d	- p d	- p d	P p d	P p d	P p d
$Fe(OH)_2$(aq)	- p d	- p d	- p d	- p d	- p d	- p d	- p d	- p d
$Fe(OH)_3^-$(aq)	- p d	- p d	- p d	P p d	P p d	P p d	P p d	P p d
$Fe(OH)_4^{2-}$(aq)	P p d	P p d	P p d	P p d	P p d	P p d	P p d	P p d
Fe^{3+}(aq)	P p d	P p d	P p d	- - -	- - -	- - -	- - -	- - -
$FeOH^{2+}$(aq)	- p d	P p d	P p d	P p d	P p d	P p d	- - -	- - -
$Fe(OH)_2^+$(aq)	- - d	- p d	- p d	P p d	P p d	P p d	P p d	P p d
$Fe(OH)_3$(aq)	- - d	- - d	- - d	- - d	- - d	- - d	- p d	- p d
$Fe(OH)_4^-$(aq)	- p d	- p d	P p d	P p d	P p d	P p d	P p d	P p d
FeO_4^{2-}(aq)	P p d	P p d	P p d	P p d	P p d	P p d	P p d	P p d

which is reported to be slow at low temperatures, but fast at high temperatures. This reaction can also be written as

$$3Fe(OH)_2(cr) \rightarrow Fe_3O_4(cr) + 2H_2O(l) + 2H^+ + 2e^-,$$

because it is actually an electrochemical reaction. However, our calculations indicate that the Schikorr reaction is not a correct way of representing the mechanism of the formation of magnetite in high temperature water as the iron(II) hydroxide is not thermodynamically stable above ~85°C. This result is in fair agreement with Linnenbom,[98] and Le and Gali.[55] The former found experimentally that ferrous hydroxide does not exist at $T = 60$°C, and the calculations of Le and Gali gave a temperature limit of 65°C.

Pourbaix diagrams for solutions with the low concentration of 10^{-8} M display soluble iron(II) species, between the immunity and passivity regions, see Fig. 3. The existence of a corrosion region between the immunity and passivity areas has not been reported earlier. The high purity philosophy in high temperature water containing steel systems can be detrimental if the potential falls into this region.

As mentioned above, ferrous hydroxide is oxidized at higher potentials to magnetite or iron(III) hydroxide, hematite or goethite, see Fig. 2. Increasing the potential oxidizes magnetite to hematite, which dissolves at very high potentials to form Fe(VI), possibly $Fe(OH)_4^{2-}$. However, this ion is probably not formed in neutral and acidic solutions, as mentioned above. As it is well known, the oxyhydroxide α-FeOOH (goethite) and the hydroxide of iron(III) are not stable at any temperature with respect to hematite. However, if haematite is excluded from the calculations, goethite becomes stable, with a stability area slightly smaller than hematite. From the thermodynamic point of view hematite formation is more stable compared to goethite when in equilibrium with aqueous solutions. Reported experimental existence of both species in the same system indicates that goethite formation is perhaps favoured for kinetic reasons. From the practical point of view, the choice of oxide or oxihydroxide of Fe(III) to be considered in a given system may also have to be based on non-thermodynamic arguments.

In alkaline solutions iron dissolves and forms ferrous and ferric anionic complexes, $Fe(OH)_3^-$, $Fe(OH)_4^{2-}$ and $Fe(OH)_4^-$, respectively. No previously published Pourbaix diagram contains more than the three first hydrolysis steps of iron, with one exception,[55] which contains four hydrolysis steps in the ferric series, but not in the ferrous. In acidic solutions and at higher potentials ferrous iron oxidizes to Fe^{3+} and $FeOH^{2+}$. The ferric ion appears in the diagrams only at 25–100°C at pH > 0.

All the aqueous complexes appear in the predominance diagrams for dissolved species in the temperature range studied, with the exception of Fe^{3+} which predominates at $T \leq 100$°C, see Fig. 4.

CONCLUSIONS

The revised Pourbaix diagrams at 25–300°C and concentrations for dissolved species of 10^{-6} and 10^{-8} M show that:

1. $Fe(OH)_2(cr)$ is stable at $T \leq 85$°C, and therefore the Schikorr reaction is not thermodynamically possible above this temperature;
2. $Fe(OH)_3(cr)$ and goethite are not stable at any temperature;
3. Haematite is the stable solid of Fe(III);

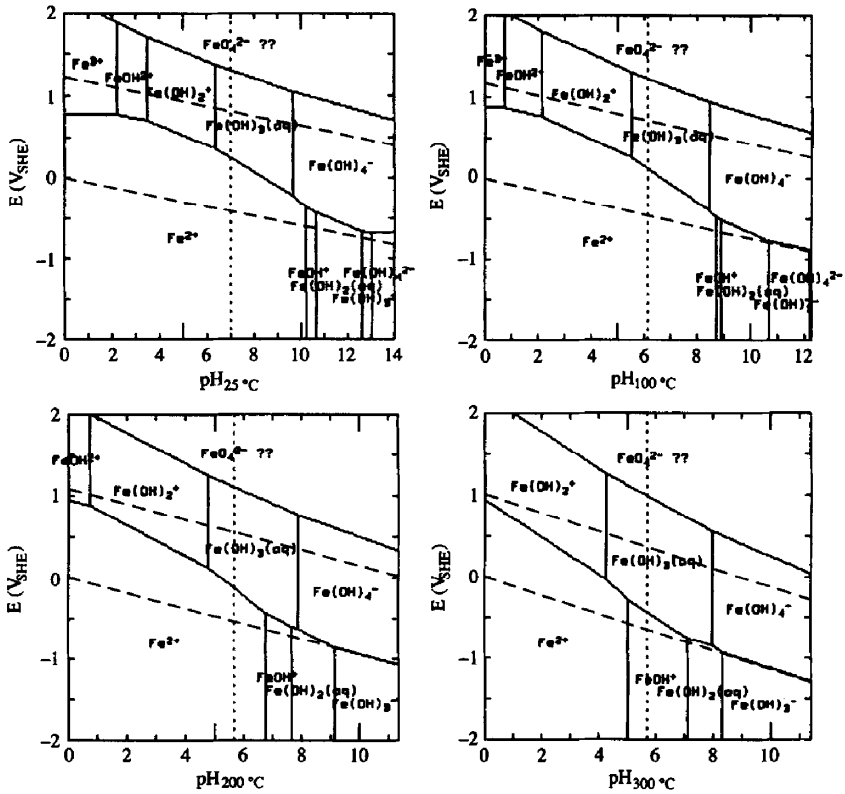

Fig. 4. Predominance diagrams for dissolved iron species at Pourbaix diagram for iron at 25, 100, 200 and 300°C.

4. Fe^{3+}(aq) is only stable at 25–100°C at pH≥0;
5. A corrosion region exists between iron and magnetite in high purity water (10^{-8} M), due to the hydrolysis steps of Fe(II).

Acknowledgements—Thanks are due to S.-O. Pettersson for his skillful computer and editorial help and to Drs Pourbaix for their useful comments. This work has been sponsored by the Swedish Nuclear Power Utilities.

REFERENCES

1. M. Pourbaix, *Thermodynamique des Solutions Aqueuses Diluées. Représentation Graphique du Rôle du pH et du Potentiel*, Ph. D. Thesis, Technische Hogeschool Delft (1945), Arnold, London (1965).
2. P. Delahay, M. Pourbaix and P. van Rysselberghe, *J. Chem. Ed.* **27**, 683 (1950).
3. R. M. Garrels, *Minerals Equilibria at Low Temperature and Pressure*, Harpers Geosciences Series, NY (1960).
4. M. Pourbaix and N. de Zubov, *Atlas d'Equilibres Electrochimiques* (ed. M. Pourbaix). Gauthier-Villars and Cie, Paris (1963).
5. R. M. Garrels and C. L. Christ, *Solutions, Minerals and Equilibria*. Freeman, San Francisco, CA (1965).
6. K. B. Krauskkopf, *Introduction to Geochemistry*. McGraw-Hill, NY (1979).
7. E. D. Verdink, *Corrosion* **12**, 371 (1967).
8. M. Pourbaix, *Werkstoffe Korr.* **20**, 773 (1969).
9. H. E. Townsend, *Corr. Sci.* **10**, 343 (1970).

10. V. Ashworth and P. J. Boden, *Corr. Sci.* **10**, 709 (1970).
11. P. A. Brook, *Corr. Sci.* **11**, 389 (1971).
12. D. Lewis, *J. Inorg. Nucl. Chem.* **33**, 2121 (1971).
13. D. Lewis, AB Atomenergi, Report Ae-424, Nyköping, Sweden (1971).
14. D. Lewis, AB Atomenergi, Report Ae-431, Nyköping, Sweden (1971).
15. D. Lewis, AB Atomenergi, Report Ae-432, Nyköping, Sweden (1971).
16. M. Pourbaix, *Handbook on Corrosion Testing* (ed. W. H. Ailor), p. 661 (1971).
17. R. J. Biernat and R. G. Robins, *Electrochem. Acta.* **17**, 1261 (1972).
18. N. G. Klyuchnikov, I. G. Gorichev and L. V. Malov, *Russ. J. Phys. Chem.* **47**, 473 (1973).
19. T. E. Markovic, *Métaux Corros. Ind.* **48**, 50 (1973).
20. T. Misawa, *Corr. Sci.* **13**, 659 (1973).
21. M. Pourbaix, *Lectures on Electrochemical Corrosion.* Plenum Press, NY (1973).
22. D. Lewis, *Chem. Script.* **6**, 49 (1974).
23. M. Pourbaix, CEBELCOR, Rappt. Tech., 126, RT 226 (1975).
24. M. Pourbaix, *J. Electrochem. Soc.* **123**, 25C (1976).
25. M. H. Froning, M. E. Shanley and E. D. Verink, *Corr. Sci.* **16**, 371 (1976).
26. L. Ahrnbohm and D. Lewis, Atomenergi, A. B., Report Ae-514, Nyköping, Sweden (1977).
27. J. D. Hem, *Geochim. Cosmochim. Acta* **41**, 527 (1977).
28. D. D. Macdonald and B. C. Syrett, *Corrosion* **35**, 471 (1979).
29. P. B. Linkson, B. D. Phillips and C.-D. Rowles, *Corr. Sci.* **19**, 613 (1979).
30. D. D. Macdonald and J. B. Hyne, Report AECL-5811, Atomic Energy of Canada Ltd (1979).
31. D. D. Macdonald, B. C. Syrett and S. S. Wing, *Corrosion* **35**, 1 (1979).
32. J. A. Revetllat and J. M. Costa, *Rev. Ibroam. Corr. Prot.* **12**, 41 (1981).
33. M. Pourbaix, A. Pourbaix and X. Z. Yang, Report EPRI-NP-2177, Appendix B1, Electric Power Research Institute, Palo Alto, CA (1981).
34. D. C. Silverman, *Corrosion* **38**, 453 (1982).
35. X. Z. Yang, Proc. 22nd CEFA–NATO Seminar, Brussels (1981).
36. H. Hirano, M. Mayuzumi and T. Kurosawa, *Boshoku Gijutsu* **31**, 517 (1982).
37. C. M. Chen and K. Aral, Report EPRI-NP-3137, Vol. 1, Electric Power Research Institute, Palo Alto, CA (1983).
38. C. M. Chen, K. Aral and G. J. Theus, Report EPRI-NP-3137, Vol. 2, Electric Power Research Institute, Palo Alto, CA (1983).
39. R. Nishimura and N. Sato, *Nippon Kinzoku Gakkashi* **47**, 1086 (1983).
40. B. Mazza and P. Pedeferri, *84 Riunione Annuale Papers Associazione Elettrotecncia ed Elettronica Italiana*, paper A30. Cagliari, Italy (1983).
41. U. Rohlfs and H. Kaesche, *Maschinenschaden* **57**, 11 (1984).
42. H. Hirano and T. Kurosawa, *Boskoku Gijutsu* **34**, 92 (1985).
43. C. W. Bale, A. D. Pelton and W. T. Thompson, *Computer Aided Aquisition and Analysis of Corrosion Data* (ed. M. W. Kendig), p. 165 (1985).
44. D. R. Drewes, *J. Chem. inf. Comput. Sci.* **25**, 73 (1985).
45. P. L. Daniel and S. L. Harper, Report EPRI-NP-4831, Electric Power Research Institute, Palo Alto, CA (1986).
46. S. J. Lennon and F. P. A. Robinson, *Corr. Sci.* **26**, 995 (1986).
47. Y. Imay, K. Osato and I. Nakauchi, *Boshoku Gijutsu* **36**, 195 (1987).
48. D. Cubicciotti, *Corrosion* **44**, 875 (1988).
49. D. Cubicciotti, *CORROSION/88*, Paper No. 254, NACE, Houston, TX (1988).
50. D. Cubicciotti, *J. nucl. Mater.* **167**, 241 (1989).
51. S. M. El-Raghy and M. F. El-Demerdsah, *J. Electrochem. Soc.* **136**, 3647 (1989).
52. G. H. Kesall and D. J. Robbins, *J. Electroanal. Chem.* **283**, 135 (1990).
53. P. Paine, *Corrosion* **46**, 19 (1990).
54. H. Yokoawa, N. Sakai, T. Kawada and M. Dokiya, *J. Electrochem. Soc.* **137**, 388 (1990).
55. H. H. Le and G. Ghali, *J. Appl. Electrochem.* **23**, 72 (1993).
56. C. M. Criss and J. W. Cobble, *J. Am. Chem. Soc.* **86**, 5385 (1964).
57. A. J. deBethune, T. S. Licht and N. Swendeman, *J. Electrochem. Soc.* **106**, 616 (1959).
58. A. J. deBethune, *J. electrochem. Soc.* **107**, 829 (1960).
59. J. C. Tanger IV and H. C. Helgeson, *Am. J. Sci.* **288**, 19 (1988).

60. E. L. Shock, E. H. Oelkers, J. W. Johnson, D. A. Sverjensky and H. C. Helgeson, *J. chem. Soc., Faraday Trans.* **88**, 803 (1992).
61. E. L. Shock and H. C. Helgeson, *Geochim. Cosmochim. Acta* **52**, 2009 (1988). Errata: **53**, 215 (1989).
62. G. Bohnsack, *The Solubility of Magnetite in Water and in Aqueous Solutions of Acid and Alkali*. Vulkan, Essen (1987).
63. P. R. Tremaine and J. C. Leblanc, *J. Solution Chem.* **9**, 415 (1980).
64. C. F. Baes Jr and R. E. Mesmer, *The Hydrolysis of Cations*. Wiley, New York (1976).
65. F. A. Cotton and G. Wilkinson, *Advanced Inorganic Chemistry*. Wiley, New York (1976).
66. U. R. Evans, *The Corrosion and Oxidation of Metals: Scientific Principles and Practical Applications*, p. 24. Arnold, London (1960).
67. D. D. Wagman, W. H. Evans, V. B. Parker, R. H. Schumm, I. Halow, S. M. Bailey, K. L. Churney and R. L. Nuttall, *J. Phys. Chem. Ref. Data* **11**, Suppl. No. 2 (1982).
68. O. Kubaschewski, C. B. Alcock and P. J. Spencer, *Materials Thermochemistry*, 6th Edn. Pergamon, Oxford (1993).
69. B. S. Hemingway, *Am. Mineral.* **75**, 781 (1990).
70. R. A. Robie, B. S. Hemingway and J. R. Fisher, *U.S. Geol. Surv. Bull.* **1452**, 0 (1978).
71. O. Knacke, O. Kubaschewski and K. Hesselmann (eds), *Thermochemical Properties of Inorganic Substances*, 2nd Edn. Springer, Berlin (1991).
72. D. K. Nordstrom, L. N. Plummer, D. Langmuir, E. Busenberg, H. M. May, B. F. Jones and D. L. Parkhurst, *Chemical Modeling of Aqueous Systems* (eds D. C. Melchior and R. L. Bassett), ACS Symposium Series 416, Vol. 2, p. 398. American Chemical Society, Washington, DC (1990).
73. J. D. Cox, D. D. Wagman and V. A. Medvedev, *CODATA Key Values for Thermodynamics*. Hemisphere, New York (1989).
74. A. Saul and W. Wagner, *J. Phys. Chem. Ref. Data* **18**, 1537 (1989).
75. D. G. Archer and P. Wang, *J. Phys. Chem. Ref. Data* **19**, 371 (1990).
76. H. C. Helgeson, *Am. J. Sci.* **285**, 845 (1985).
77. J. W. Larson, P. Cerutti, H. K. Garber and L. G. Hepler, *J. Phys. Chem.* **72**, 2902 (1968).
78. E. E. Bernarducci, L. R. Morss and A. R. Miksztal, *J. Solution Chem.* **8**, 717 (1979).
79. D. O. Whittemore and D. Langmuir, *J. Chem. Engng Data* **17**, 288 (1972).
80. K. E. Heusler and W. J. Lorenz, *Standard Potentials in Aqueous Solution* (eds A. J. Bard, R. Parsons and J. Jordan), p. 391. Marcel Dekker, New York (1985).
81. J. A. Bolzan and A. J. Arvía, *Electrochim. Acta.* **8**, 375 (1963).
82. G. K. Johnson and J. E. Bauman, *Inorg. Chem.* **17**, 2774 (1978).
83. C. F. Baes and R. E. Mesmer, *Am. J. Sci.* **281**, 935 (1981).
84. R. S. Sapieszko, R. C. Patel and E. Matijevic, *J. Phys. Chem.* **81**, 1061 (1977).
85. Y. Zeng, R. Ai and F. Wang, *Geochim. Cosmochim. Acta* **53**, 1875 (1989).
86. R. H. Wood, *J. Am. Chem. Soc.* **80**, 2038 (1958).
87. G. Carlot, A. Collumeau and M. J. C. Marchon, *Selected Constants. Oxidation–Reduction Potentials of Inorganic Substances in Aqueous Solution*. Butterworths, London (1971).
88. E. L. Shock, H. C. Helgeson and D. A. Sverjensky, *Geochim. Cosmochim. Acta.* **53**, 2157 (1989).
89. I. Puigdomenech, Report TRITA-OOK-3010, Department of Inorganic Chemistry, The Royal Institute of Technology, Stockholm (1983).
90. G. Eriksson, *Anal. Chim. Acta* **112**, 375 (1979).
91. V. I. Zarembo, A. A. Slobodov, V. G. Kritskii, L. V. Puchkov and V. M. Sedov, *J. Appl. Chem. USSR* **59**, 951 (1986).
92. S. E. Ziemniak, *J. Solution Chem.* **21**, 745 (1992).
93. Y. Zeng, R. Ai and Y. Chen, *Sci. Sinica (B)* **24**, 1221 (1986).
94. B. Beverskog, Report Studsvik/M-91/52, Restricted distribution. (1992).
95. M. Cohen, *Corrosion Chemistry* (ed. R. F. Gould,), ACS Symposium Series No. 89, p. 126. American Chemical Society, Washington, DC (1979).
96. G. Schikorr, *Z. Elektrochem.* **25**, 65 (1929).
97. G. Schikorr, *Z. Anorg. Allg. Chem.* **212**, 33 (1933).
98. V. J. Linnenbom, *J. Electrochem. Soc.* **105**, 322 (1958).